THE STRENGTHS AND WEAKNESSES OF INVERTED PENDULUM MODELS OF HUMAN WALKING

Michael McGrath[1], David Howard[2], Richard Baker[1]

[1]School of Health Sciences, University of Salford, M6 6PU, UK;

[2]School of Computing, Science and Engineering, University of Salford, M5 4WT, UK.

Email: m.p.mcgrath@edu.salford.ac.uk

Keywords: Inverted pendulum, gait, walking, modelling

Word count: 3024

Abstract – An investigation into the kinematic and kinetic predictions of two "inverted pendulum" (IP) models of gait was undertaken. The first model consisted of a single leg, with anthropometrically correct mass and moment of inertia, and a point mass at the hip representing the rest of the body. A second model incorporating the physiological extension of a head-arms-trunk (HAT) segment, held upright by an actuated hip moment, was developed for comparison. Simulations were performed, using both models, and quantitatively compared with empirical gait data. There was little difference between the two models' predictions of kinematics and ground reaction force (GRF). The models agreed well with empirical data through mid-stance (20-40% of the gait cycle) suggesting that IP models adequately simulate this phase (mean error less than one standard deviation). IP models are not cyclic, however, and cannot adequately simulate double support and step-to-step transition. This is because the forces under both legs augment each other during double support to increase the vertical GRF. The incorporation of an actuated hip joint was the most novel change and added a new dimension to the classic IP model. The hip moment curve produced was similar to those measured during experimental walking trials. As a result, it was interpreted that the primary role of the hip musculature in stance is to keep the HAT upright. Careful consideration of the differences between the models throws light on what the different terms within the GRF equation truly represent.

Introduction

As far as the authors have been able to ascertain the first mention of the term "inverted pendulum" (IP) as a model of the stance phase of walking was by Cavagna et al. [1] although similar concepts can be traced much earlier [2-4]. More recently the IP has formed the basis of a growing body of work associated with the Dynamic Walking movement [5] which is based on principles first elucidated by Mochon and McMahon [6] and subsequently by Tad McGeer [7, 8]. Recent work of this group has tended to focus on the transitions from one step to the next [9-11]. The group, as well as other researchers, have also presented many extended versions of IP models including springs, dampers, telescopic actuators, additional segments and joints. [12-16].

This work has focussed on energetics and stability whereas the kinematics and kinetics of movement are more relevant to most clinical biomechanists and is less well understood. The mechanics of the IP mechanism itself (as opposed to the transitions), were presented briefly by Anderson and Pandy [appendix of 17], and gave a brief description of the ground reaction force (GRF) under an IP. A more comprehensive comparison with gait data by Buczek et al. [18] concluded that the IP predicts the anterior velocity of the whole body centre-of-mass (CM) and anterior component of the GRF reasonably well but not the vertical components.

The aim of this paper is thus to build on the work of Buczek et al [18] in extending the ideas of the Dynamic Walking Group into the domain of clinical biomechanics. This includes extending their analysis to include fast and slow walking speeds, and extending the IP model to include a hip joint controlled by a joint actuator in such a way as to maintain an upright head-arms-trunk (HAT) segment. This will be done by starting the HAT segment with zero

angular velocity and calculating the moment so that there is zero angular acceleration. Doing this throughout the simulation will ensure there is no angular motion of the HAT. Whilst this is unlikely to affect the overall dynamics of the system (it is still a one degree-of-freedom system) it will allow an investigation of the effects of the hip flexor and extensor muscles. There is considerable current interest in the decomposition of the GRF to investigate the function of different muscles [17, 19, 20] and the analysis of the IP model has been extended to evaluate the contribution of the hip actuator to the GRF.

Method

Figure 1a shows the free body diagram for the simple IP model. The inertial properties of the IP have been altered from the previous models [18] in that the *'leg'* has been assigned a mass (m_1), with CM at a point a given distance (d_1) from the pivot, and moment of inertia (I_1). This change was motivated by the desire for the mass properties of the leg to be the same in both models to avoid an associated confounding effect. The mass of the rest of the body (m_2) acts through a single point at the *'hip joint'*, a given distance (l_1) from the pivot. The mass at the hip has no moment of inertia which is equivalent to assuming that it is concentrated at a single point as assumed in other simple IP models [18, 21]. The anterior-posterior direction is defined as the *x* axis and the vertical direction is defined as the *y* axis.

Using information taken from Winter [22, 23], all data regarding lengths, distance and mass distributions were taken for a person of 1.80m height and 80 kg mass. The position of the IP was specified by the angle that its axis of symmetry makes with the vertical (θ_1).

The equations of motion for the IP were derived, as were the equations for the horizontal and vertical components of the GRF (see Appendix). In order for this to be done, the two masses were equated to a single mass (m) with a given moment of inertia (I), acting at a given distance from the pivot (d_t).

Figure 1b shows the free body diagram for the HAT model which consists of two segments of lengths l_1 and l_2. The inertial properties of the two segments are specified by the respective masses (m_1 and m_2), which are located at defined distances from the distal ends of the segments (d_1 and d_2), and moments of inertia (I_1 and I_2). The positions of each segment are specified by the angles that their longitudinal axes make with the vertical (θ_1 and θ_2). A hip moment, M, is applied at the joint between the two segments. The equations of motion for the HAT model can be derived, as can the formulae for the horizontal and vertical components of the GRF (see Appendix).

From the equations of motion, M is calculated so as to enforce the constraint that the HAT segment's angular acceleration equals zero. With the values of M and $\ddot{\theta}_2$, the system is reduced to a single equation of motion that is used to calculate $\ddot{\theta}_1$.

The lengths l_1 and l_2, the distribution of mass between m_1 and m_2, the CM positions on their segments, d_1 and d_2, and the moments of inertia, I_1 and I_2, were all selected using Winter's data [22, 23].

The same source was used for gait data against which the output of the simulations was judged. These cover a range of walking speeds and average temporal spatial parameters. The simulations represented the half-gait cycle from the middle of one double support phase (at 5% of the gait cycle) to the middle of the next (at 55% of the gait cycle). All Winter's data are thus time normalized to this definition of a step.

The equations of motion of the two models were integrated numerically over 0.001s intervals, using a Taylor expansion method. The leg segment in both models was assumed to move through an arc of $2\theta_{1_{initial}}$symmetrical about the vertical. This meant that the final angle of $\theta_1$was equal and opposite to the initial angle. This was set to ensure the required average step length for the experimental data ($2l \sin \theta_{1_{initial}}$). The initial velocity was then optimised to ensure that the time taken to move through this arc resulted in the required cadence (note that this also constrains the average walking speed). All graphical output was time normalized to step duration.

Inverse dynamics were subsequently performed using a standard Newton-Euler approach. This provided validation for the forward dynamic calculations, as well as allowing a comparison of the moments acting about the *'hip'* in each of the models.

An examination of the GRFs constituent parts was also undertaken. The terms in the GRF equations were separated and the forces attributable to *'gravitational'*, *'centripetal'* and *'muscular'* effects were calculated.

Results

Figure 2 represents the components of hip velocity at the three different walking speeds for the IP and HAT models. Differences between the models are almost indiscernible graphically, particularly the vertical velocity curves, emphasising how close the results are to one another. The RMS values in Table 1 confirm that differences are always less than or equal to 0.03m/s.

The way the horizontal velocity varied across the gait cycle followed the same patterns observed in the experimental data (see Table 1). During mid-stance (20-40% of the gait cycle) the vertical velocity also shows a good match between the predicted and experimental data (within 1.44 standard deviations at all walking speeds).

The models' vertical velocities are equal and opposite at the beginning and end of the step cycle which is inconsistent with a cyclic walking pattern and would require an infinite instantaneous acceleration in the vertical direction at the transition from one step to the next. The predicted data differ from the experimental values over the first and last quarters of the step (half gait cycle). This shows that the models do not account for the mechanisms the body uses to control foot velocity at initial contact and thus avoid a discontinuity in velocity, allowing for a smooth cyclic pattern. Evidence in clinical biomechanics, as well as slip resistance research, suggests that the knee begins to flex just prior to ground contact, at times resulting in a negative horizontal velocity of the heel and an associated brief forward GRF, as well as a positive vertical GRF arresting the downward motion of the heel at contact. These nuances will not be addressed by a simple IP, but neither are they critical to the overall performance of these IP and HAT models.

The RMS values in Table 1 (column a) showed that the two sets of predictions of hip velocity and the GRF are close to one another. As expected, the incorporation of joint actuation in this model has made little difference to the overall dynamics of movement.

Figure 3 presents the GRFs at different walking speeds for the IP and HAT models, in the horizontal and vertical directions. All plots include the decomposition into gravity and centripetal components for the IP model, and gravity, centripetal and muscle moment components for the HAT model (see Appendix for definitions).

The total GRF components for the IP and HAT models appear similar and this is confirmed by the RMS values in Table 1 (column a). A difference between the two models can be observed once the individual GRF components are evaluated. As expected the centripetal component varies minimally between the two models and the gravitational component differs by an RMS of 2.16% bodyweight (BW). It is hypothesised that this difference between the results of the two models is likely due to the action of the hip joint moment.

There is a good match with the experimental data for the horizontal component of the total GRF predicted for both models (within 1.45 standard deviations for all walking speeds). The match for the vertical component, however, varies up to 3.75 standard deviations. It is still reasonable during mid-stance (within 1.26 standard deviations) but poor over the first and fourth quarter of the step (up to 4.33 standard deviations difference). This provides further evidence that the IP model is a weak simulation of double support and the step-to-step transition. One final observation is that over the first and fourth quarters of the step, as walking speed increased, the correlation with experimental data became weaker.

Hip joint moment graphs can be produced for both models by applying inverse dynamics and they can be compared to experimental data (Figure 4). For all walking speeds, the IP model has zero moment about the hip. This is because the mass at the hip has zero moment of inertia. For the HAT model, the moment varies from an extensor moment at the start of the cycle to a flexor moment of equal magnitude at the end. This matches the broad pattern

seen in the experimental data with the magnitude at natural speed within 0.48 standard deviations.

Discussion

The aim of this study was to further investigate what insights simple IP based models can give us into the mechanisms that drive human walking. The IP model of walking has been described as the "simplest walking model" [24]. Despite this only one previous paper has set out to describe the biomechanical characteristics of the IP and then only at a single walking speed [18]. Adding a HAT segment held upright by an actuator (representing the hip extensor musculature) is a simple modification that can make the model more physiologically representative and provide insight into the role of hip muscles during walking.

The horizontal component of GRF was predicted well by both models throughout the stance phase. Researchers often make the assumption that in early stance and particularly in the push-off phase, muscle activity is required to generate the distinctive shape of the horizontal component of the GRF [25]. The results of the IP model show that, to an extent, this is a natural consequence of the body's posture and this behaviour of the horizontal GRF will be present regardless of whether muscles are present or not.

The most novel aspect of the HAT model was the inclusion of a hip moment, calculated to keep the HAT segment upright. The resulting hip moment curves matched those measured in practical experiments well (within 1.34 standard deviations), particularly at natural walking speed. From these results it could be hypothesised that the primary purpose of the hip moment being to maintain the upright posture of the trunk and therefore illustrating

how even a simple anatomical extension to the IP model can provide extra insight into gait mechanics. The predicted contribution of hip musculature to the GRF is different to the findings of Anderson and Pandy [17]. They stated that hip extensors contributed up to 40% BW in early single support. On the other hand they found that the hip flexors provided minimal contribution, anywhere throughout single stance. The differences may be attributed to the model dependency of 'induced accelerations' (IA) as highlighted by Chen [26] who said that changing the assumptions or number of DOFs in the model, can have a marked impact on the resulting IA values.

One of the biggest failures of the models is that they are not inherently cyclic. The vertical component of CM velocity is upwards at the start of the step and downwards at the end. A number of studies have addressed the step-to-step transition issue [5, 9-11, 27-29] assuming that it leads to a collision during which energy is lost. The empirical data, however, particularly for the vertical component of the CM velocity, show considerable departures from model predictions over the first and last quarters of the step resulting in minimal vertical velocity at the start and end of the step. The implication here is that the IP is not a good model of how the body moves at the beginning and end of the step rather than that there is an inevitable collision as a consequence of IP like movement.

Another limitation of these models becomes apparent upon observing the vertical component curves of the GRF which are always below bodyweight. The IP models thus do not satisfy the first pre-requisite of normal walking – adequately supporting bodyweight. The average vertical force under either foot is about 10% less than bodyweight. Empirical data show the characteristic double bump of the vertical component of the GRF which IP models cannot predict [17]. This emphasizes the importance of double support, during which

the forces under both limbs add to give the highest overall force on the body at any time during the gait cycle, as a mechanism for ensuring bodyweight is supported. Differences between the models and empirical data increase with increasing walking speed suggesting that the IP becomes a less good model of walking as speed increases.

There are also more obvious limitations to these models. Firstly, during normal walking, the distance between the hip and the pivot is not a constant distance. This is a known problem with IP models which has led to the development of Spring Loaded Inverted Pendulum (SLIP) models [15, 30]. Secondly, the lack of an ankle joint nullifies the push and pull control the ankle muscles are able to produce in order to stabilise the motion of the leg. Finally, the interaction with the ground is assumed to be a workless constraint, at a single point. This assumption ignores the motion of the centre of pressure (COP) underneath the foot.

Decomposing the GRF into its constituent parts is a relatively new technique [17] and is still poorly understood. We have analysed this for two very simple models and it is here where the largest differences are observed between the two models with the "gravitational" GRF differing at the beginning and end of the step. This difference is almost exactly that which is attributed to the hip muscles in the HAT model (the centripetal component and total force are very nearly identical). Considering the free body diagram and the similarity in the way the two models move, gravity would appear to have an extremely similar effect on both models and it may be that labelling this as the "gravity" component is misleading. The difference is attributable to the different structures of the models (one has a hip joint, the other doesn't). This component is that which would be exerted by the structure in the absence of movement or muscular action and "structural support" might be considered a better label than "gravity". The explanation of the analytical results is then that the jointed

HAT structure is inherently less resistant to collapse under the same gravitational forces as the IP and muscle activity is required to allow it to move similarly.

In conclusion, consideration of these two models suggests that IP based models appear to give valuable insights into the fundamental mechanisms by which the body moves through single support. They are not cyclic, however, and cannot serve as reliable models for step-to-step transitions. Incorporating an actuated hip joint identifies the primary role of the hip musculature in stance as that of keeping the HAT upright.

References

[1] Cavagna GA, Thys H, Zamboni A. The sources of external work in level walking and running. J Physiol. 1976;262:639-57.

[2] Saunders J, Inman V, Eberhart H. The major determinants in normal and pathological gait. Journal of Bone and Joint Surgery 1953;35A:543-58.

[3] Elftman H. Biomechanics of muscle with particular application to studies of gait. Journal of bone and Joint Surgery - American. 1966;48:363-77.

[4] Alexander M. Mechanics of bipedal locomotion. In: Davis P, editor. Perspectives in experimental biology. Oxford: Pergamon; 1976. p. 493-504.

[5] Kuo AD. The six determinants of gait and the inverted pendulum analogy: A dynamic walking perspective. Human Movement Science. 2007;26:617-56.

[6] Mochon S, McMahon TA. Ballistic walking. Journal of Biomechanics. 1980;13:49-57.

[7] McGeer T. Passive dynamic walking. The international journal of robotics research. 1990;9.

[8] McGeer T. Dynamics and control of bipedal locomotion. Journal of Theoretical Biology. 1993;163:277-314.

[9] Donelan JM, Kram R, Kuo AD. Mechanical work for step-to-step transitions is a major determinant of the metabolic cost of human walking. Journal of Experimental Biology. 2002;205:3717-27.

[10] Donelan JM, Kram R, Kuo AD. Simultaneous positive and negative external mechanical work in human walking. Journal of Biomechanics. 2002;35:117-24.

[11] Kuo AD, Donelan JM, Ruina A. Energetic consequences of walking like an inverted pendulum: step-to-step transitions. Exercise and Sport Sciences Reviews. 2005;33:88-97.

[12] Srinivasan M. Fifteen observations on the structure of energy-minimizing gaits in many simple biped models. Journal of The Royal Society Interface. 2010.

[13] O'Connor S, Kuo A. Walking, Skipping, and Running Produced From a Single Bipedal Model. Conference of the American Society of Biomechanics. Palo Alto, CA, USA2007.

[14] Koolen T, Boer TD, Rebula J, Goswami A, Pratt J. Capturability-based analysis and control of legged locomotion, Part 1: Theory and application to three simple gait models. Int J Rob Res. 2012;31:1094-113.

[15] Hong H, Kim S, Kim C, Lee S, Park S. Spring-like gait mechanics observed during walking in both young and older adults. Journal of Biomechanics. 2013;46:77-82.

[16] Kim S, Park S. Leg stiffness increases with speed to modulate gait frequency and propulsion energy. Journal of Biomechanics. 2011;44:1253-8.

[17] Anderson FC, Pandy MG. Individual muscle contributions to support in normal walking. Gait & Posture. 2003;17:159-69.

[18] Buczek FL, Cooney KM, Walker MR, Rainbow MJ, Concha MC, Sanders JO. Performance of an inverted pendulum model directly applied to normal human gait. Clinical Biomechanics. 2006;21:288-96.

[19] Francis CA, Lenz AL, Lenhart RL, Thelen DG. The modulation of forward propulsion, vertical support, and center of pressure by the plantarflexors during human walking. Gait & Posture. 2013.

[20] Liu MQ, Anderson FC, Pandy MG, Delp SL. Muscles that support the body also modulate forward progression during walking. Journal of Biomechanics. 2006;39:2623-30.

[21] Kuo AD. Energetics of actively powered locomotion using the simplest walking model. Journal of biomechanical engineering. 2002;124:113-20.

[22] Winter DA. Biomechanics of Human Movement: John Wiley & Sons, Inc.; 1979.

[23] Winter DA. The biomechanics and motor control of human gait: Normal, Elderly and Pathological. 2nd ed. Waterloo: Waterloo Biomechanics; 1991.

[24] Garcia M, Chatterjee A, Ruina A, Coleman M. The simplest walking model: stability, complexity, and scaling. J Biomech Eng. 1998;120:281-8.

[25] Perry J, Burnfield J. Gait Analysis: Normal and Pathological function. Second ed. Thorofare, NJ, USA: SLACK Incorporated; 2010.

[26] Chen G. Induced acceleration contributions to locomotion dynamics are not physically well defined. Gait & Posture. 2006;23:37-44.

[27] Srinivasan M, Ruina A. Computer optimization of a minimal biped model discovers walking and running. Nature. 2006;439:72-5.

[28] Adamczyk PG, Kuo AD. Redirection of center-of-mass velocity during the step-to-step transition of human walking. Journal of Experimental Biology. 2009;212:2668-78.

[29] Donelan JM, Kram R, Kuo AD. Mechanical and metabolic determinants of the preferred step width in human walking. Proc Biol Sci. 2001;268:1985-92.

[30] Millard M, Kubica E, McPhee J. Forward dynamic human gait simulation using a SLIP target model. Procedia IUTAM. 2011;2:142-57.

Figure 1: Free body diagrams for (a) the IP model (including the calculation approximations in bold) and (b) the HAT model of the stance phase of walking.

Figure 2: The linear velocity components for the IP and HAT models at different walking speeds. The shaded areas indicate experimental data and double stance periods. The simulations represented the half-gait cycle from the middle of one double support phase (at 5% of the gait cycle) to the middle of the next (at 55% of the gait cycle).

Figure 3: The GRF predictions at different walking speeds for (a) the IP model: horizontal GRF component on the top row, vertical GRF component on the second row (b) the HAT model: horizontal GRF component on the top row, vertical GRF component on the second row. For all plots the simulations represented the half-gait cycle from the middle of one double support phase (at 5% of the gait cycle) to the middle of the next (at 55% of the gait cycle).

Figure 4: The hip joint moments (flexion positive) for the IP and HAT models (this remains zero throughout the simulation for the IP model). The simulations represented the half-gait cycle from the middle of one double support phase (at 5% of the gait cycle) to the middle of the next (at 55% of the gait cycle).

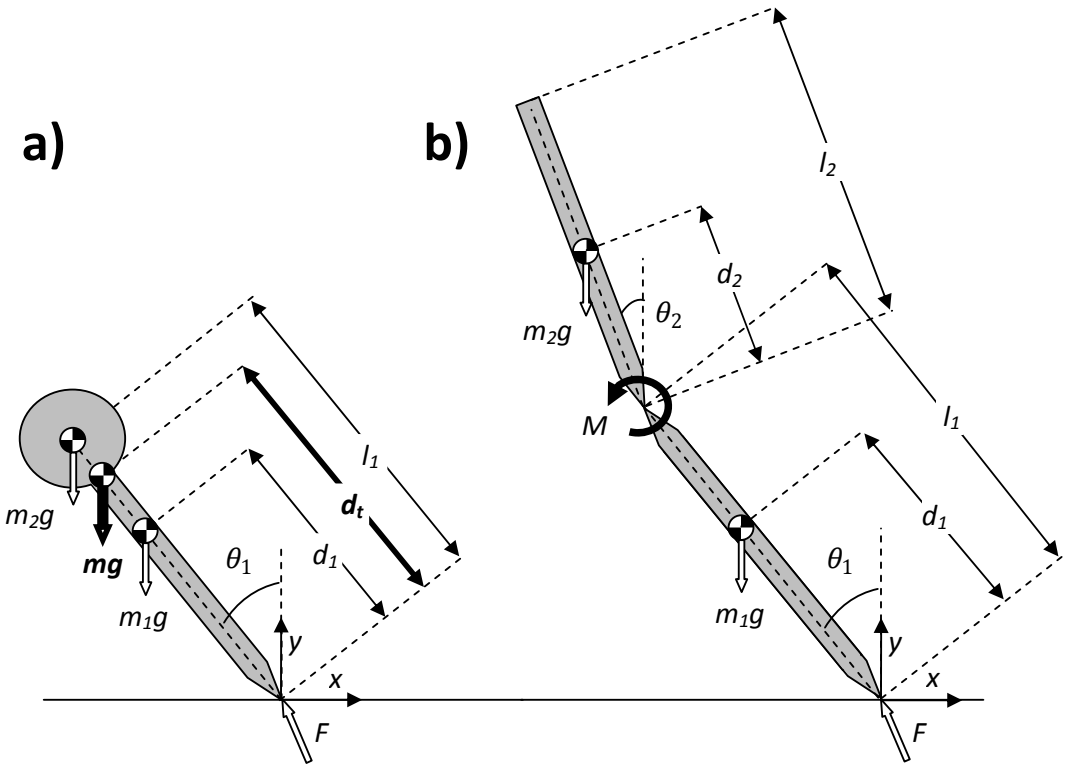
a)
b)
m_2g
mg
m_1g
l_1
d_t
d_1
θ_1
y
x
F
l_2
d_2
θ_2
M

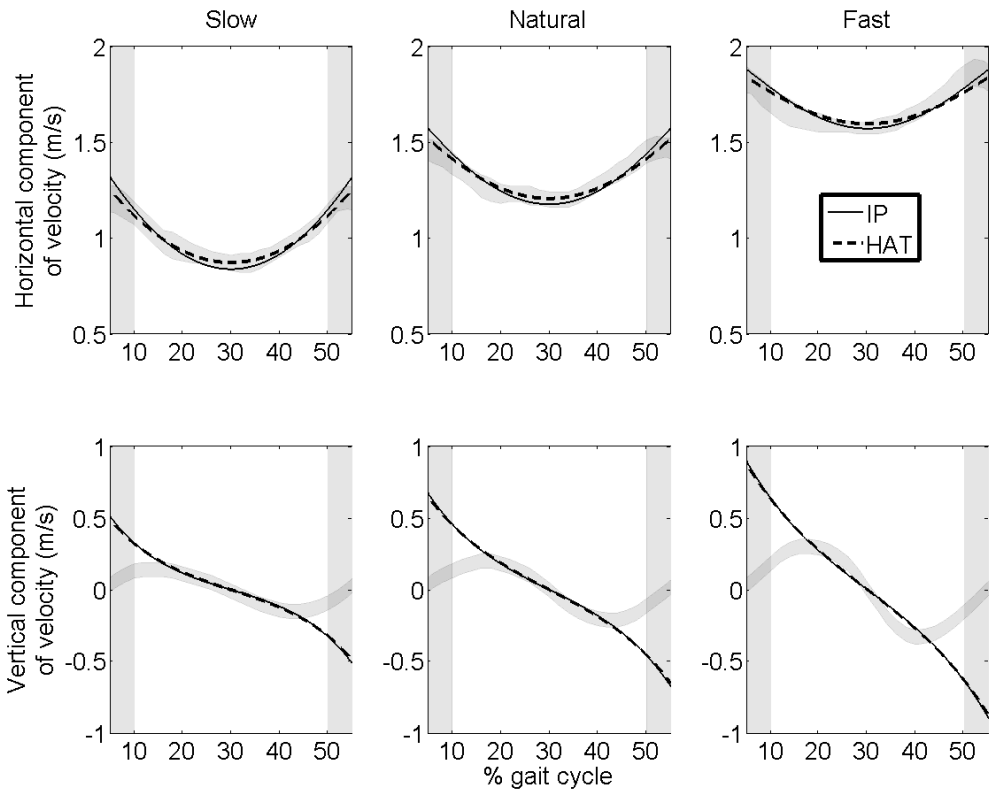
Slow
Natural
Fast
Horizontal component of velocity (m/s)
Vertical component of velocity (m/s)
% gait cycle
IP
HAT
2
1.5
1
0.5
0
-0.5
-1
10
20
30
40
50

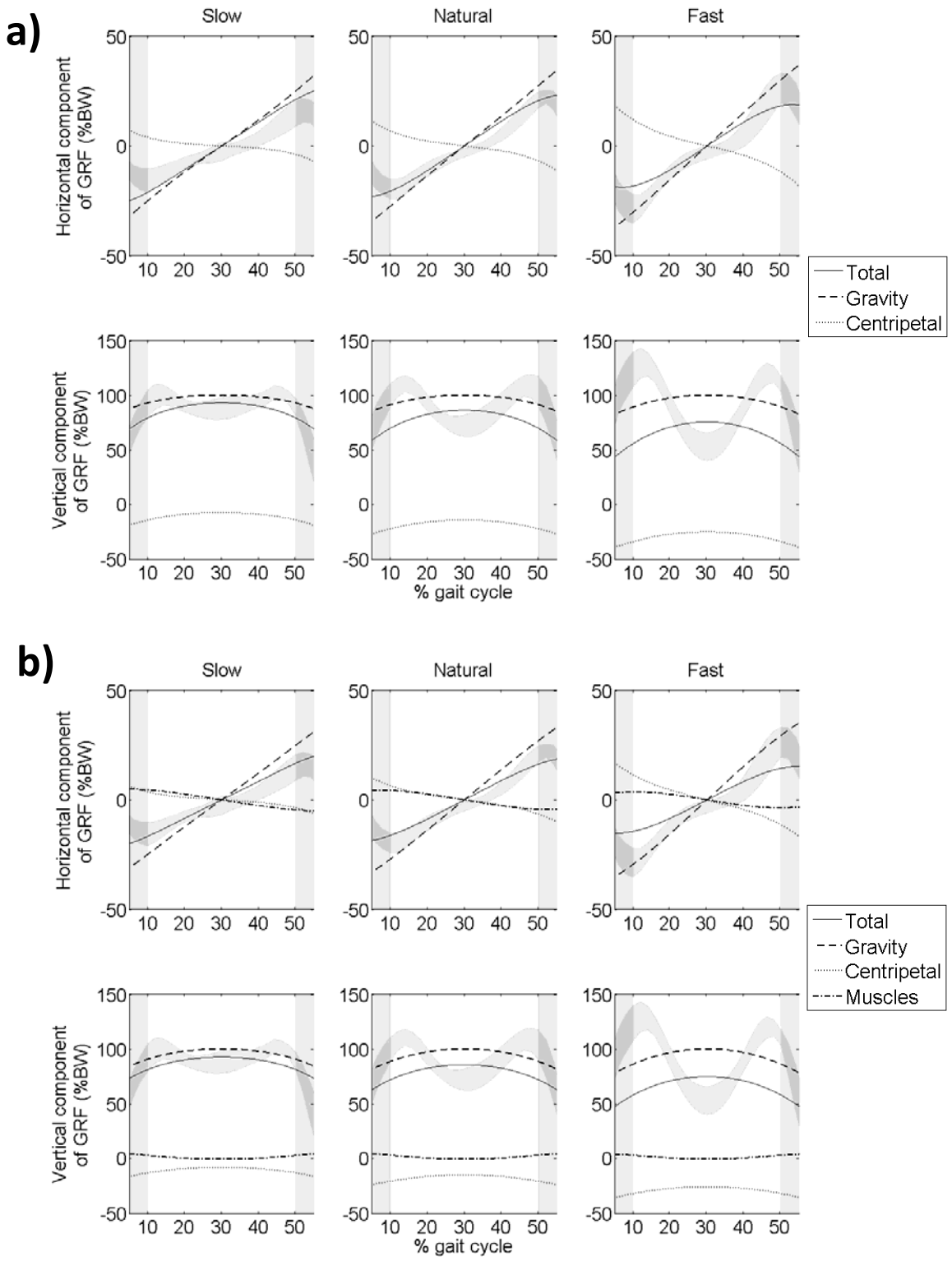
a)
Slow
Natural
Fast
Horizontal component of GRF (%BW)
Vertical component of GRF (%BW)
% gait cycle
Total
Gravity
Centripetal
b)
Slow
Natural
Fast
Horizontal component of GRF (%BW)
Vertical component of GRF (%BW)
% gait cycle
Total
Gravity
Centripetal
Muscles

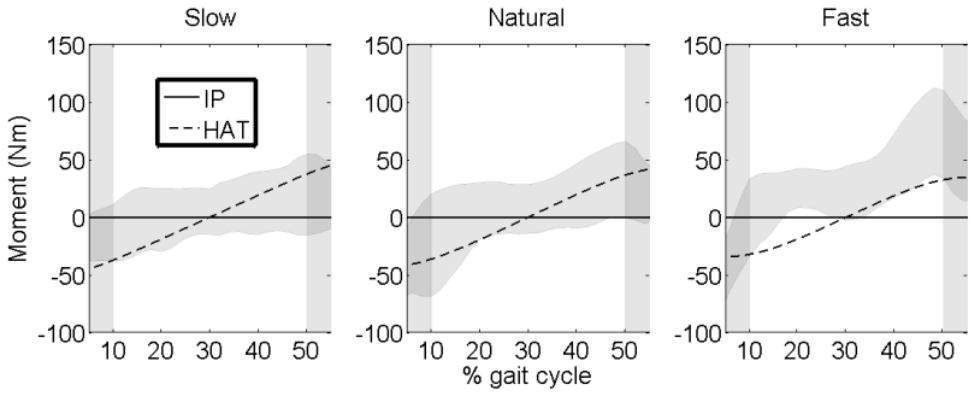
Slow
Natural
Fast
IP
HAT
Moment (Nm)
150
100
50
0
-50
-100
10
20
30
40
50
% gait cycle

			(a) IP vs HAT			(b) IP vs exp. data			(c) HAT vs exp. Data		
			Slow	Natural	Fast	Slow	Natural	Fast	Slow	Natural	Fast
Velocity		Horizontal	0.03 m/s	0.03 m/s	0.02 m/s	0.65	0.77	0.66	0.2	0.47	0.75
		Vertical	0.01 m/s	0.01 m/s	0.01 m/s	3.5	4.97	6.84	3.37	4.85	6.73
GRF	Total	Horizontal	3.18% BW	3.16% BW	2.83% BW	1.45	1.31	1.14	0.87	1.15	1.42
		Vertical	1.5% BW	1.61% BW	1.57% BW	1.19	2.17	3.75	1.13	2.08	3.65
	Gravitational	Horizontal	0.38% BW	0.45% BW	0.62% BW	-	-	-	-	-	-
		Vertical	1.6% BW	1.86% BW	2.16% BW	-	-	-	-	-	-
	Centripetal	Horizontal	0.26% BW	0.36% BW	0.52% BW	-	-	-	-	-	-
		Vertical	0.9% BW	1.14% BW	1.5% BW	-	-	-	-	-	-
Hip Moment			-	-	-	0.44	0.63	1.31	0.65	0.48	1.34

Table 1: The RMS error between (a) the IP and HAT models' predictions (given in parameter specific units) (b) the IP model's predictions and the experimental data (normalised by standard deviations) (c) the HAT model's predictions and the experimental data (normalised by standard deviations)

Appendix

In order to predict how the two models will move, their equations of motion must be derived. For known values of initial segment angle and initial angular velocity, these equations calculate the angular acceleration of the segment at that particular time instant. Using a Taylor expansion to perform a numerical integration, the segment angular acceleration can be used to evaluate the angular position and angular velocity for the next time instant. Repeating this method over and over allows the motion of the segments to be predicted over any given time span.

The method used in this study for deriving the equations of motion is known as Lagrangian mechanics and involves evaluating the kinetic and potential energies of the system.

IP Model

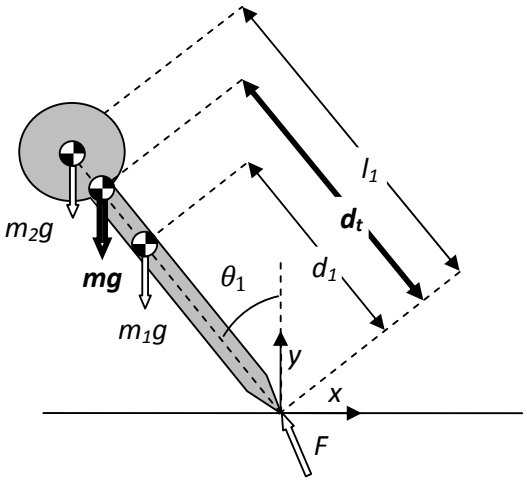

From Figure 1a

Since this IP model has two masses for a single segment, the masses and moments of inertia for both are equated to a single mass (m) and moment of inertia (I), acting at a given distance (d_t) from the pivot.

$$m = m_1 + m_2$$

Equation 1

$$d_t = \frac{(m_1 d_1 + m_2 l_1)}{(m_1 + m_2)}$$

Equation 2

$$I = (I_1 + m_1(d_t - d_1)^2) + (I_2 + m_2(l_1 - d_t)^2)$$

Equation 3

The Lagrangian is given by the potential and kinetic (both linear and rotational) energy:

$$L = T - V = \frac{1}{2} m {d_t}^2 {\dot{\theta}_1}^2 + \frac{1}{2} I {\dot{\theta}_1}^2 - mgd_t \cos\theta_1$$

Equation 4

which is differentiated to give the equations of motion:

$$\frac{d}{dt}\frac{\partial L}{\partial \dot{\theta}_1} - \frac{\partial L}{\partial \theta_1} = 0$$

Equation 5

$$\left(m{d_t}^2 + I\right)\ddot{\theta}_1 - mgd_t \sin\theta_1 = 0$$

Equation 6

$$\ddot{\theta}_1 = \frac{mgd_t}{(md_t{}^2 + \mathrm{I})} \sin\theta_1$$

Equation 7

This is decomposed into two terms. These are the acceleration due to gravity, which is a function of angular position, and the acceleration due to centripetal effects, which is a function of angular position and velocity.

$$\ddot{\theta}_1 = \frac{mgd_t}{(md_t{}^2 + \mathrm{I})} \sin\theta_1$$

Equations 8

$$\ddot{\theta}_{1C} = 0$$

Equation 9

Anderson and Pandy[18] applied Newton's law to determine the components of the ground reaction in the vertical direction and this approach can be extended to determine the horizontal component as well:

$$F_x = m\ddot{x}$$

Equations 10

$$F_y = mg + m\ddot{y}$$

Equation 11

Substituting expressions for $\ddot{x}$ and $\ddot{y}$:

$$\ddot{x} = -\ddot{\theta}_1 d_t \cos\theta + \dot{\theta_1}^2 d_t \sin\theta_1$$

Equations 12

$$\ddot{y} = -\ddot{\theta}_1 d_t \sin\theta - \dot{\theta_1}^2 d_t \cos\theta_1$$

Equation 13

Substituting for $\ddot{x}$, $\ddot{y}$ and $\ddot{\theta}_1$ gives:

$$F_x = -g\frac{m^2 {d_t}^2}{(m{d_t}^2 + I)}\cos\theta_1 \sin\theta_1 + m\dot{\theta_1}^2 d_t \sin\theta_1$$

Equation 14

$$F_y = mg - g\frac{m^2 {d_t}^2}{(m{d_t}^2 + I)}\sin^2\theta_1 - m\dot{\theta_1}^2 d_t \cos\theta_1$$

Equation 15

Terms involving g represent the effect of gravity at any particular instant and terms involving velocity represent centripetal forces[18].

$$F_{Gx} = -g\frac{m^2 {d_t}^2}{(m{d_t}^2 + I)}\cos\theta_1 \sin\theta_1$$

Equation 16

$$F_{Gy} = mg - g\frac{m^2 {d_t}^2}{(m{d_t}^2 + I)}\sin^2\theta_1$$

Equation 17

$$F_{Cx} = m\dot{\theta_1}^2 d_t \sin\theta_1$$

Equation 18

$$F_{Cy} = -m\dot{\theta_1}^2 d_t \cos\theta_1$$

Equation 19

H.A.T. Model

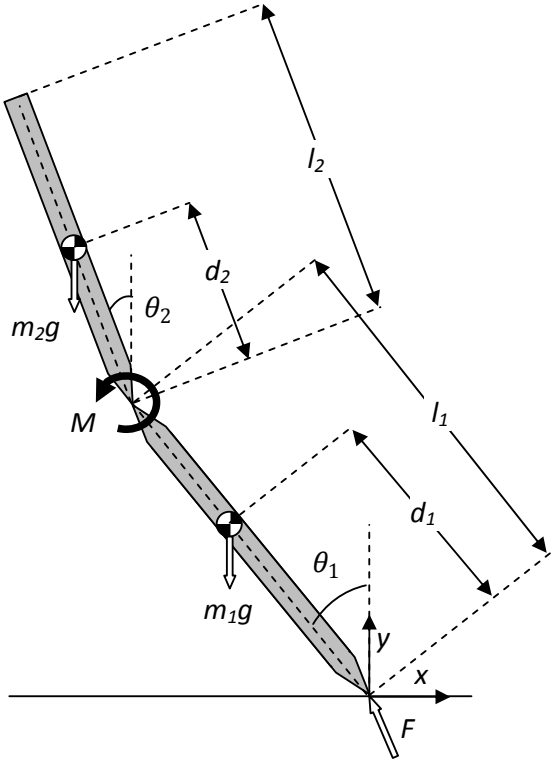

From Figure 1b

The Lagrangian for this system is:

$$L = \frac{1}{2}(m_1 d_1^2 + m_2 l_1^2 + I_1)\dot{\theta}_1^2 + \frac{1}{2}(m_2 d_2^2 + I_2)\dot{\theta}_2^2 + m_2 l_1 d_2 \cos(\theta_1 - \theta_2)\dot{\theta}_1\dot{\theta}_2$$
$$- (m_1 d_1 + m_2 l_1) g\cos\theta_1 - m_2 d_2 g\cos\theta_2$$

Equation 20

The equations of motion are given by:

$$\frac{d}{dt}\frac{\partial L}{\partial \dot{\theta_1}} - \frac{\partial L}{\partial \theta_1} = M\frac{\partial(\theta_1 - \theta_2)}{\partial \theta_1}$$

Equation 21

$$\frac{d}{dt}\frac{\partial L}{\partial \dot{\theta_2}} - \frac{\partial L}{\partial \theta_2} = M\frac{\partial(\theta_1 - \theta_2)}{\partial \theta_2}$$

Equation 22

Which we can be evaluated and written in the form:

$$\begin{pmatrix} A_{11} & A_{12} \\ A_{21} & A_{22} \end{pmatrix}\begin{pmatrix} \ddot{\theta}_1 \\ \ddot{\theta}_2 \end{pmatrix} = \begin{pmatrix} B_1 \\ B_2 \end{pmatrix}$$

Equation 23

Where:

$$A_{11} = (m_1 d_1^2 + m_2 l_1^2 + I_1)$$

$$A_{22} = (m_2 d_2^2 + I_2)$$

$$A_{12} = A_{21} = m_2 l_1 d_2 \cos(\theta_1 - \theta_2)$$

$$B_1 = -m_2 l_1 d_2 \sin(\theta_1 - \theta_2)\dot{\theta}_2^2 + (m_1 d_1 + m_2 l_1) g \sin\theta_1 + M$$

$$B_2 = m_2 l_1 d_2 \sin(\theta_1 - \theta_2)\dot{\theta}_1^2 + m_2 d_2 g \sin\theta_2 - M$$

From $\begin{pmatrix} A_{11} & A_{12} \\ A_{21} & A_{22} \end{pmatrix}\begin{pmatrix} \ddot{\theta}_1 \\ \ddot{\theta}_2 \end{pmatrix} = \begin{pmatrix} B_1 \\ B_2 \end{pmatrix}$

Equation 23, M is calculated so as to enforce the constraint that the angular acceleration of segment *2* is zero. Knowing the value of M leads to a single equation of motion to calculate the angular acceleration of segment *1*. This is integrated numerically. Using the same

method as the IP model, this acceleration is divided into gravity, centripetal and muscle terms.

The vertical component of F can be expressed in terms of linear vertical accelerations:

$$F_y - mg = m_1\ddot{y}_1 + m_2\ddot{y}_2$$

Equation 24

$$\ddot{y}_1 = d_1\left(-\ddot{\theta}_1\sin\theta_1 - \dot{\theta}_1{}^2\cos\theta_1\right)$$

Equation 25

$$\ddot{y}_2 = d_2\left(-\ddot{\theta}_2\sin\theta_2 - \dot{\theta}_2{}^2\cos\theta_2\right) + l_1\left(-\ddot{\theta}_1\sin\theta_1 - \dot{\theta}_1{}^2\cos\theta_1\right)$$

Equation 26

The horizontal component of F was calculated using the same method.

$$F_x = ma = m_1\ddot{x}_1 + m_2\ddot{x}_2$$

Equation 27

$$\ddot{x}_1 = d_1\left(-\ddot{\theta}_1\cos\theta_1 + \dot{\theta}_1{}^2\sin\theta_1\right)$$

Equation 28

$$\ddot{x}_2 = d_2\left(-\ddot{\theta}_2\cos\theta_2 + \dot{\theta}_2{}^2\sin\theta_2\right) + l_1\left(-\ddot{\theta}_1\cos\theta_1 + \dot{\theta}_1{}^2\sin\theta_1\right)$$

Equations 29

To decompose the GRF into gravitational, centripetal and muscular terms, the B_1 and B_2 terms in Equation 23 were separated:

$$\begin{pmatrix} A_{11} & A_{12} \\ A_{21} & A_{22} \end{pmatrix} \begin{pmatrix} \ddot{\theta}_1 \\ \ddot{\theta}_2 \end{pmatrix} = \begin{pmatrix} B_{1\mathrm{G}} \\ B_{2\mathrm{G}} \end{pmatrix} + \begin{pmatrix} B_{1\mathrm{C}} \\ B_{2\mathrm{C}} \end{pmatrix} + \begin{pmatrix} B_{1\mathrm{M}} \\ B_{2\mathrm{M}} \end{pmatrix}$$

Equation 30

Where:

$$B_{1_G} = (m_1 d_1 + m_2 l_1) g \sin\theta_1, \qquad B_{2_G} = -m_2 d_2 g \sin\theta_2$$

$$B_{1_C} = -m_2 l_1 d_2 \sin(\theta_1 - \theta_2)\dot{\theta}_2^2, \qquad B_{2_C} = m_2 l_1 d_2 \sin(\theta_1 - \theta_2)\dot{\theta}_1^2$$

$$B_{1_M} = M, \qquad B_{2_M} = -M$$

B1 and *B2* terms in *A*11*A*12*A*21*A*22*θ*1*θ*2=*B*1*B*2

Equation 23 calculates the angular accelerations

Equation 24

$$\ddot{y}_1 = d_1 \left(-\ddot{\theta}_1 \sin\theta_1 - \dot{\theta}_1{}^2 \cos\theta_1 \right)$$

Equation 25

$$\ddot{y}_2 = d_2 \left(-\ddot{\theta}_2 \sin\theta_2 - \dot{\theta}_2{}^2 \cos\theta_2 \right) + l_1 \left(-\ddot{\theta}_1 \sin\theta_1 - \dot{\theta}_1{}^2 \cos\theta_1 \right)$$

-29 will give the GRF due to these accelerations.